

Numerical and experimental investigations of laser shock forming aluminum alloy sheet with mold

Xingquan Zhang¹ · Yan Zhang¹ · Yiwei Zhang² · Shanbao Pei¹ · Zhilai Huang¹ · Lei Deng³ · Shengzhi Li²

Received: 11 October 2016 / Accepted: 6 December 2016 / Published online: 27 December 2016
© Springer-Verlag France 2016

Abstract Laser shock forming (LSF) technology employs shock waves to form sheet metal into three-dimensional complex parts, and has application potential in manufacturing sheet metal parts. In this paper, the forming of 2024 aluminum alloy sheet with LSF was investigated through numerical and experimental methods. The numerical model was established with the commercial code ABAQUS/Explicit. The formed conical cup was obtained from the simulation, and validated by the experiment. With the verified numerical model, the deformation behaviors, including deformation velocity, sheet thickness variation and strain distribution, were studied. In addition, the influence of different shock wave pressures on the forming precision was also investigated. The experimental and numerical results show that the metal sheet loaded by shock wave can take the shape of the mold, and the non-uniform thickness is distributed in the formed cup. The investigations also display that there exists reverse deformation at the central region of deforming sheet owing to severe collision during LSF. In order to obtain formed part with better quality, an appropriate pressure of applied shock waves is required.

Keywords Laser shock forming (LSF) · Deforming velocity · Strain distribution · Thickness variation · Shock wave pressure

Introduction

Nowadays, aluminum alloy sheet is a candidate material used in closure panels and structural components in aerospace, automotive industries and so on, which is attributed to its low density and moderate strength. However, the viability of the conventional press forming at room temperature is hindered by its poor formability. Previous investigations have indicated that the formability of aluminum alloy increases dramatically when sheet is shaped by high-speed techniques, such as electrohydraulic forming [1], explosive forming [2] and electromagnetic forming [3, 4]. Laser shock forming (LSF) is an ultrafast sheet forming technique that the plastic deformation is accomplished in the level of nanoseconds [5], so it can be served as a potential technique to overcome the inherent formability limitations in aluminum alloy. LSF forms metallic sheet with shock wave, which is induced by a precise-controlled laser pulse. Compared with traditional sheet stamping [6, 7], the forming momentum in LSF is from shock wave pressure other than hydraulic pressure, and its forming pressure is up to several GPa level, which is far higher than the pressure supplied by the hydraulic system, so it can deform high strength metallic sheet. The mold employed in LSF is simple, and only a semi-mold (female die) is needed. As a result, there is no difficulty in controlling and adjusting the clearance between the male die and the female die, which always exists in traditional sheet punch forming. Furthermore, the sheet forming with LSF is completed within a considerably short time, which can save the production time

✉ Xingquan Zhang
zhxq@ahut.edu.cn

¹ School of Mechanical Engineering, Anhui University of Technology, Ma'anshan, Anhui 243002, China

² School of Material Science and Engineering, Anhui University of Technology, Ma'anshan, Anhui 243002, China

³ State Key Laboratory of Material Processing and Die & Mould Technology, Huazhong University of Science and Technology, Wuhan, Hubei 430074, China

and cost greatly. Considering these advantages, LSF becomes a superior alternative to the conventional sheet forming technology in fabricating high-strength sheet components in the fields of electronics, aerospace, biomedical engineering and so on.

During the process of LSF, the surrounding region of metal sheet is constrained by blank holder, and the sheet is dragged into the mold cavity by the momentum obtained from the shock wave. The mold is often used to control 2D size of deformed metal sheet other than depth size, and the depth of formed parts is determined by the laser parameters such as laser fluence, pulse duration, spot size, and the number of pulses other than the mold, so the deformed part displays a shape of bulge [5, 8–10]. Apart from the above-mentioned 2D LSF, the mold is also employed to control 3D size of deformed metal sheet, and the sheet can be formed into an expected shape which is consistent with the shape of the designed mold. Obviously, the parts formed by 3D LSF possess higher forming precision and wider application in practice. Therefore, the 3D LSF has attracted more and more attention of manufacturers and researchers [11–13]. Shen et al. [14] probed into the flexible rubber material as a soft punch driven by laser-induced shock wave to form the sheet. LSF takes place in the scale of nanoseconds and belongs to the high-speed forming [5, 9, 11]. These investigations are of great use for understanding the characteristics of LSF. However, the previous references touched on 3D LSF paid few attentions to the velocity of sheet deformation and the collision between the metal sheet and the mold, which play an important role in sheet forming precision. They rarely explored the effect of applied shock wave pressure on sheet forming precision either. Therefore, some deformation behaviors of metal sheet during LSF are still unknown. Consequently, the technology of 3D LSF needs to be researched continuously to get more insights into the forming mechanism, which can eventually prompt it into practice.

In this paper, the numerical model of laser shock forming 2024 aluminum alloy sheet with mold was established using the commercial code ABAQUS/Explicit. The Fabbro's model was employed to estimate the peak pressure of shock wave. The Johnson-Cook model was used to consider the effect of strain rate on the material flow behaviors. The deformation behaviors of sheet metal impacted by laser-induced shock wave were predicted, which included the transient velocity, strain distribution and thickness variation. The influence of shock wave pressure on sheet forming precision was also investigated. As a means of validation, the forming experiments were carried out, and the physical shapes of the formed sheets were also measured in the experiments.

Experimental procedure

Experiment preparation and instruments

Figure 1 is a schematic illustration of LSF with mold. The experiments of sheet shock forming were implemented by utilizing the Q-switched Nd-YAG pulsed laser processing system. The laser was placed in a closed room to avoid dust pollution, and the generated pulse was first delivered to the shock operation room by the total internal reflection light pipe. Subsequently, the pulse passed through convergent lens and transparent confinement overlay, and finally was focused on central region of metal sheet. The temporal profile of the pulse approximated the Gaussian shape, and its spatial profile was modulated to a nearly flat shape. Laser operated at 1 Hz frequency, the emitted pulse with wavelength of 1064 nm, the full width at half maximum (FWHM) of laser pulse of about 20 ns, and local laser spot 3 mm in diameter.

The material of mold was Cr12MoV steel (in National Standard of PRC). The mould was quenched after metal cutting and the hardness was 58–62 HRC after quenching. The designed dimensions of mold were shown in Fig. 2. The outer diameter of mold 20 mm, the draw angle 30°, the depth of the mold cavity 0.8 mm, the width of the mold cavity 4 mm, fillet radius 0.3 mm at mold cavity entrance and 0.2 mm at mold cavity bottom corner, and a small vent with 0.6 mm in diameter at the bottom of the mold. The sheet surface to be irradiated was first covered by a professional adhesive black tape with thickness 50 μm , which was served as an ablative overlay. The sheet metal was then placed onto the top surface of rigid mold and clamped tightly by a blank holder and two bolts. The mold together with sheet was fixed to a clammer, which was driven by means of an anthropomorphic robot.

Prior to laser shocking, the sheet metal to be formed was immersed into the flowing water, which was used as the confinement overlay. During laser shocking, the laser pulse passed through the confinement overlay of water with thickness of 2 mm, and irradiated onto the surface of ablative layer of black tape. The ablative material was vaporized instantly and ionized into the high pressure plasma. The diffusion of high pressure plasma led to shock waves, which were imposed on the surface of metal sheet and pushed sheet metal into the mold cavity. After laser shocking, the remaining layer of ablated tape was removed from the deformed sheet surface, and the metal surface was then cleaned with alcohol. Subsequently, a high-resolution upright motorized digital microscope (Olympus DSX510) was employed to measure the 3D morphology of the deformed sheet, and the 2D profiles of the convex surface on deformed sheets were also measured. An optical microscope was used to measure its thickness. In order to measure the cross-sectional thickness of formed part accurately, the deformed part was first cut by wire electric

Table 1 Mechanical properties of Al2024-T351

Material	Density (kg/m ³)	Young modulus (GPa)	Yield stress (MPa)	Elongation at fracture (%)	Poisson ratio
Al 2024-T351	2780	72	360	19	0.33

pulse employed in the experiment was about 20 ns, as presented in “Experiment preparation and instruments” section, so the FWHM of shock wave could set to be 70 ns. The pressure–time curves of laser shock waves with four different pressures were plotted in following Fig. 3.

Velocity and momentum

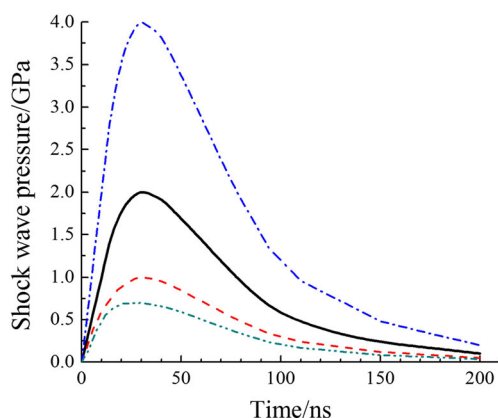
In order to analyze the loading conditions of metal sheet subjected to shock wave, a rectangular coordinate system was established, as displayed in Fig. 4. The axis of applied laser beam overlapped the z -axis, and the direction of shock wave pressure was downward. The shock wave is induced by laser and its spatial pressure is often non-uniform [16], such as Gaussian spatial distribution, and the shock pressure at one point is a function of time t and the radial distance r , so the shock pressure can be expressed as $P(r, t)$. At the moment t , the incremental momentum dI can be expressed with the pressure $P(r, t)$ and the incremental distance dr . It can be defined as:

$$dI = 2\pi r \cdot p(r, t) dr dt \quad (2)$$

Then, the total momentum I of sheet obtained from the shock waves can be given:

$$I = \int_0^{r_0} \int_0^{\tau} 2\pi r \cdot p(r, t) dr dt \quad (3)$$

where r_0 is the diameter of the laser spot, and τ is the duration of shock wave.

**Fig. 3** Profiles of temporal pressures of shock waves

When the shock wave pressure is distributed uniformly in laser spot, the above Eq. (3) is simplified into the function of time t only, namely $p(r, t) = p(t)$, so total momentum I also equals

$$I = \pi r_0^2 \int_0^{\tau} p(t) dt \quad (4)$$

Under the action of shock wave pressure, an initial velocity of metal sheet is v_0 . Then

$$I = mv_0 = \rho V v_0 = \rho \pi r_0^2 h v_0 \quad (5)$$

where m is the mass of sheet beneath laser spot, h is the sheet thickness, and ρ is the density.

Thus, from Eqs. (4) and (5), the initial velocity of the impacted region can be calculated as:

$$v_0 = \frac{\int_0^{\tau} p(t) dt}{h \rho} \quad (6)$$

Therefore, the initial velocity of metal sheet is proportional to the imposed pressure and inversely proportional to the thickness.

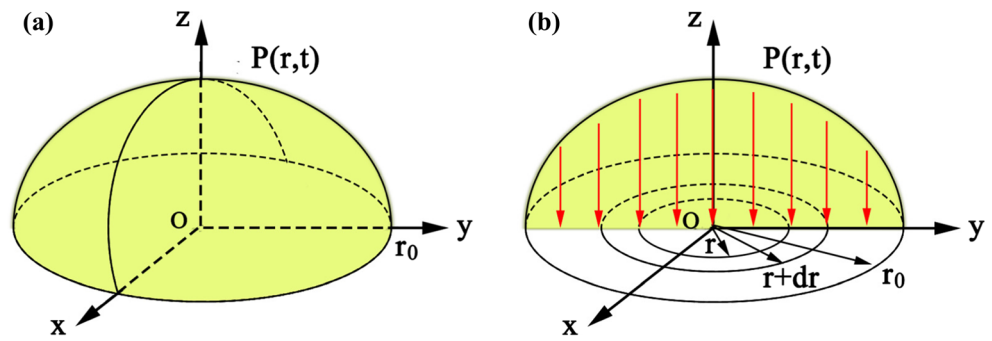
Stress–strain constitution

Since the material subjected to laser shocking accomplishes plastic deformation within a very short time, the high strain rate changes the material behaviors significantly. In order to consider the influence of strain and strain rate on the sheet plastic forming, the simplified Johnson–Cook constitutive model proposed by Johnson and Cook [17] is adopted due to the negligible heat effect on metal sheet during instant laser irradiation, as given in following Eq. (7)

$$\sigma = [A + B(\varepsilon)^n] \left[1 + C \ln \left(\frac{\dot{\varepsilon}}{\varepsilon_0} \right) \right] \quad (7)$$

where σ is the dynamic yield strength, ε and $\dot{\varepsilon}$ are the equivalent plastic strain and the equivalent plastic strain rate respectively, ε_0 denotes the reference strain rate. A stands for the yield stress under quasi-static condition, B and n are the strain hardening coefficient, C represents the strain rate hardening coefficient. The parameters of Al2024-T351 alloy used in Johnson–Cook model were listed in Table 2.

Fig. 4 Illustration of shock wave pressure distribution. **a** 3D spatial distribution of shock wave pressure, **b** 2D distribution of shock wave pressure



Numerical simulation of LSF

The commercial code ABAQUS, including the codes ABAQUS/Explicit and ABAQUS/Implicit, was widely used to predict the laser-induced residual stress in previous works [10, 18]. Compared with ABAQUS/Implicit, the code ABAQUS/Explicit runs robustly in handling the dynamic response of the material and the frictional contact problem [11]. In the present work, the code ABAQUS/Explicit was also utilized to develop numerical model to analyze the dynamic response of metal sheet as well as the complicated interaction between the mold and sheet.

The dimensions of sheet metal in simulation were the same as those in previous tests. Due to a symmetrical distribution of loading and the geometric construction, a one-half finite element model instead of an entire one was used to reduce the computing cost, as depicted in Fig. 2. During the meshing, two type elements were employed to meet the needs of different requirements. Solid element C3D8R, a 8-node linear brick with reduced integration and hourglass, was used to mesh sheet metal to describe accurately the behaviors of metal deformation during LSF, and it was also applied to the blank holder. Solid element C3D10M, a 10-node modified quadratic tetrahedron, was selected to mesh the mold with complex geometry. During simulation, both the blank holder and the mold were set as rigid bodies. Boundary condition, *Encastre*, was selected from load module and applied to restrict all degrees of freedom of the nodes in the bottom of mold and blank holder. In addition, it was necessary to consider the contact conditions between the sheet and the mold as well as the sheet and the blank holder. According to the previous reference [11], the value of friction coefficient was set to be 0.05 in the tangential behavior.

Results and discussion

Finite element model verification

Figure 5a shows the surface image of the coating ablated by laser with power density of 2.34 GW/cm². It can be clearly seen that the top thin layer of coating within laser spot is ablated and some debris of black coating still adheres to the peripheral of laser spot owing to shock wave transverse flow. The remaining ablative coating protects metallic material from heat damage resulted from laser irradiation, which has been described by [19, 20]. Figure 5b and c present the deformed metal sheet after laser shock. It can be found that the flat sheet is shaped into a conical cup. The surfaces of cup display no signs of melting, burning or ablation, which manifests that the forming process is pure mechanical not thermal [21, 22]. Compared with the spherical-bottom bulge obtained from LSF without mold, the conical cup with a flat bottom is obtained in current case, which indicates that sheet metal under the action of shock wave pressure can take the geometrical shape of the mold. At present, due to the local laser spot smaller than the mold hole, it is difficult to ensure that two centers overlap entirely during laser shocking, so the center of area loaded by the shock wave pressure does not overlap that of mold cavity, and the sheet deforms asymmetrically. Therefore, the profile of deformed part cross-section presents a little asymmetry, as displayed in Fig. 5c and Fig. 5d displays the 3D morphology and 2D cross-sectional profile of the formed cup. It is noteworthy that the bottom width of the formed cup is about 2250 μm and the maximum depth reaches approximately 831 μm, which approximately equals to the depth of mold cavity. Figure 5e reveals the predicted 3D contour and the cross-sectional profile of the cup with FEM. From

Table 2 Johnson-Cook parameters of Al 2024-T351

Material	A (MPa)	B (MPa)	C	n	$\dot{\epsilon}_0$
Al 2024-T351	369	684	0.0083	0.73	1

Fig. 5 A comparison between simulated and experimental part formed by laser with power density 2.34 GW/cm^2 . **a** surface image of ablated layer after irradiation; **b** appearance of surface subjected to laser; **c** appearance of surface opposite to laser irradiation; **d** the profile of central cross section of formed part; **e** the predicted shape of central cross section of formed part

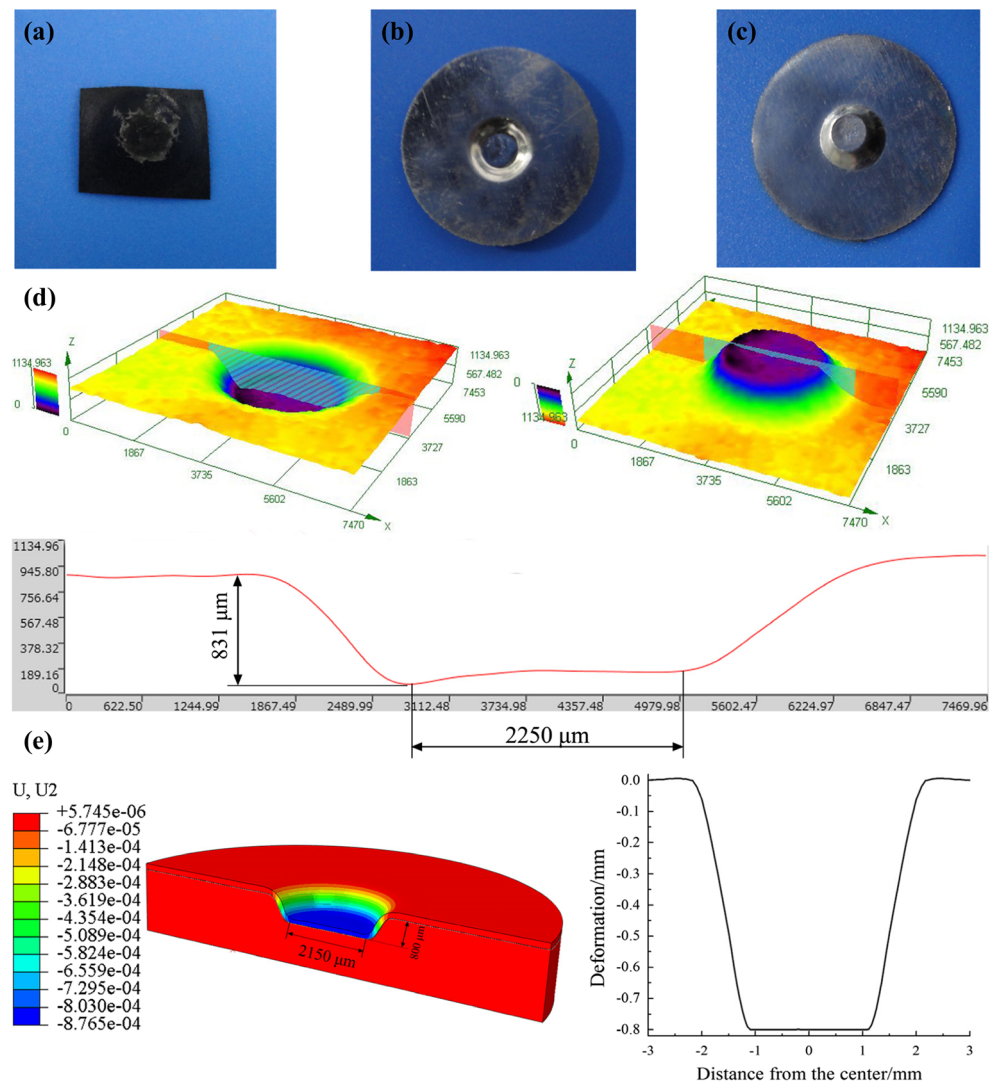


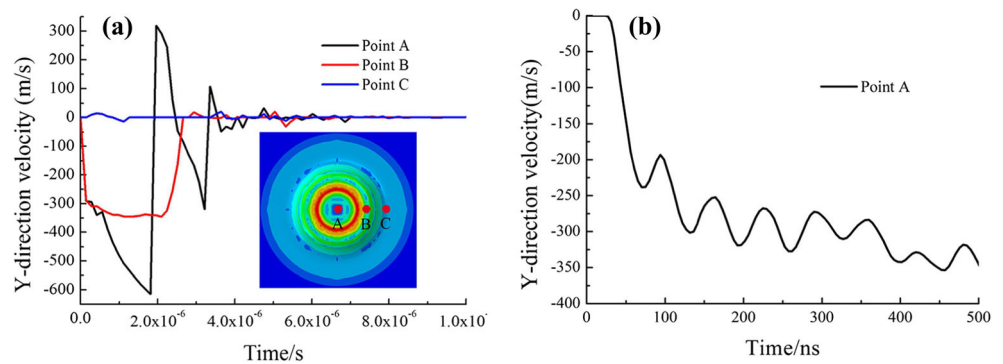
Fig. 5e, it can be seen that the predicted maximum depth of the cup is $800 \mu\text{m}$, 3.73% smaller than the test value, and the predicted bottom width is $2150 \mu\text{m}$, 4.44% smaller than the experimental value. The error values are within allowable range in practical application. The deviation is mainly attributed to the discrepancy between the applied pressure of shock wave and the calculated one. Generally speaking, the physical experimental cup is correlated well with that obtained from the numerical model. Hence, the developed finite element model is validated.

Velocity

In order to evaluate the movement of sheet metal during LSF, three typical points at the bottom surface of sheet are selected. Point A is situated at the center of metal sheet. Point B and C are located at positions 1.2 and 2.2 mm away from the sheet center respectively, and their

corresponding locations are the bottom corner and the upper entrance of mold cavity. Figure 6a shows the velocities of typical points in sheet shocked by with power density 2.34 GW/cm^2 . As can be seen, the downward velocity of point A in the initial stage is as fast as 614 m/s. At 1840 ns, point A suddenly moves upward, and the velocity is up to 319 m/s, which indicates that the sheet collides severely with the mold cavity and bounces off. After several collisions, its velocity decreases to 0 m/s gradually owing to the exhaustion of kinetic energy obtained from shock waves. At point B, the maximum downward velocity reaches up to 300 m/s. After impact against the mold cavity, the bouncing velocity declines rapidly to 0 m/s. At point C, the velocity is extremely slow, and point C lags behind point A and B in movement. It is interesting to notice that the velocity of point C is first upward and then downward. The phenomenon cannot appear during the traditional sheet stamping forming.

Fig. 6 Velocity histories of typical points at the bottom surface of sheet metal. **a** three typical points in whole time; **b** point A in initial period of 500 ns



The upward velocity is attributed to the transverse elastic expansion of metal material, which incurs from the transverse stress wave propagation induced by laser shocking.

When sheet metal is subjected to shock waves, it obtains a certain momentum from shock wave, and the central impacted region first moves downward rapidly. Due to the continuity of the sheet material, the zone next to the impacted region is dragged from previously moving material, and subsequently moves downward. With the expansion of moving region, the mass of sheet material participating in movement increases, and the corresponding velocity decreases according to the conservation of momentum. Therefore, it is reasonable that the velocity of point A is the fastest while the velocity of point C is the slowest. In the same way, due to point C far away from sheet center, it needs more time for transverse stress wave to arrive there, so the starting moving time of point C is put off.

During the sheet moving downward in initial stage, the kinetic energy obtained from shock wave converts gradually into plastically dissipated energy, elastically stored energy and so on. With increase in the plastic deformation, kinetic energy gradually decreases, plastically dissipated energy gradually increases, and elastically stored energy gradually increases. When the central region of metal sheet first collides with the mold cavity, it does not stop moving due to its high speed, but jumps up. During the sheet moving upward, the kinetic energy goes on converting into plastically dissipated energy, elastically stored energy and so on. When the central point A stops moving upward, it reaches the maximum height, and its instantaneous velocity is 0. Since a large number of elastic energy has been stored in deformed sheet at this time, it will be released and convert into kinetic energy. As a result, the metal sheet keeps on moving, but the direction of velocity changes downward owing to sheet elastic shrinkage. Subsequently, the central region collides with mold cavity bottom again. Compared with the first collision, the collision strength of the second collision subsides significantly, and the jump-up speed and jumped height are dropped prominently, because the vast majority of kinetic energy from shock wave has been consumed in the form of plastic work. The collision and friction also consume some kinetic energy. When the point A reaches the peak height at the second time, the elastic energy

stored during the second jumping is released and makes central point A move down once again. Compared with the location of point A, point C is close to the sidewall of mold cavity and the blank holder, so it moves difficultly because of the constrain. Therefore, there exists that point C is static while point A is still moving, point A does not move until the kinetic energy is consumed up.

Figure 6b shows the velocity of central point A within the initial period of 500 ns. It can be seen that the velocity of point A is always increased to 240 m/s in the initial period of 80 ns, and then fluctuates slightly, but the general trend of velocity is increased, and finally reaches 614 m/s at the period of 1840 ns as illustrated in Fig. 6a. It is well known that when the shock wave is imposed on the surface of metal sheet and the compressive stress wave is induced and propagates into material, so the velocity is increased in initial stage. When the compressive stress wave arrives at the back free surface of metal sheet, it is reflected and turned into the tensile stress wave. Since the direction of tensile stress wave is opposite to the direction of initial velocity, the velocity of point A is decreased. When the tensile stress propagates to the initially propagating surface, it will be converted into compressive stress wave again, which accelerates the material particle. The back-and-forth propagations of stress wave in metal sheet lead to slight fluctuation of the velocity. As the above presentation, the zone near the impacted region also generates movement downward during LSF, which results in increasing of velocity of point A according to the composition of velocities. Therefore, the general trend of point A velocity is increased in spite of its fluctuating. Peyre et al. [23] had used a Doppler-laser velocimeter system, a velocity interferometer system for any reflector (VISAR), to measure the velocity of central node at the back-free surface of the 200 μm thick aluminum foil impacted by laser with 4 GW/cm². The velocity of the central point is always increased to about 320 m/s in the initial stage, which is much higher than that in present work, because the pressure of applied shock wave is stronger than that employed in current case and the dynamic yield strength of pure aluminum used in their work is much lower than that of Al 2024-T351. However, the shape of velocity-time curve in initial stage in the experiments is very similar to the predicted one in our current case, which

validates the predicted velocity. Due to the complexity of metal sheet shocked by laser, the deforming velocity of metal sheet still needs further investigation.

Strain distribution

Figure 7 illustrates the contours of strain distributions in metal sheet before collision and after fitting the mold cavity. It can be found from Fig. 7 that most regions in sheet metal are subjected to tensile strain in the radial direction and compressive strain in the axial direction. When metal sheet is irradiated by laser, the material beneath laser spot is first compressed intensely by shock wave, and undergoes shearing around laser spot edge [10]. Then, metal sheet bulges towards the mold cavity because of inertia effect. The material at the entrance of mold cavity experiences bending, stretching, initial shearing and even necking, but the material outside the mold hole cannot flow into the mold cavity due to the confinement of the holder, so the significant strain gradient occurs at the edge of laser spot and the mold cavity entrance. During LSF, the sheet plastic deformation depends on the reduction in thickness and the elongation in radial and tangential directions. When metal sheet collides with the mold cavity, the material at the bottom of deformed sheet undergoes huge compressive stress and gets squeezed successively from the center of mold cavity to its sidewalls as “inertial ironing”. Therefore, the material is subjected to compressive strain in the axial direction and tensile strain in radial direction owing to the principle of constant volume. The strain distributions in the deformed sheet before

collision in present study are well consistent with the results in previous laser bulge forming [24].

Thickness distribution

Figure 8 reveals a comparison between the numerical and experimental thickness distribution. The thickness distribution of deformed sheet is characterized by thickness thinning percentage using Eq. (8)

$$e_t = \frac{t_0 - t}{t_0} 100\% \quad (8)$$

where e_t is the thinning percentage, t denotes the final thickness, and t_0 stands for the initial thickness.

During LSF, due to the confinement of blank holder, the material within the mold cavity undergoes bending, stretching and even necking owing to momentum effects, so the thickness of the deformed sheet is reduced generally. However, the magnitude of thickness reduction at different regions is different, and the thickness of the formed cup is non-uniform, as illustrated in Fig. 8. According to previous Fig. 6, we know that the central region of bulge first impacts on mold cavity bottom with the fastest speed. The severest impact leads to the material flowing radially from the central region to outer surrounding regions. As a result, the thickness at the central region of cup bottom is reduced to 0.148 mm from the original 0.2 mm. Because of the surrounding region moving downward slowly in comparison with the central region, the surrounding region of sheet is stretched slightly, so the less

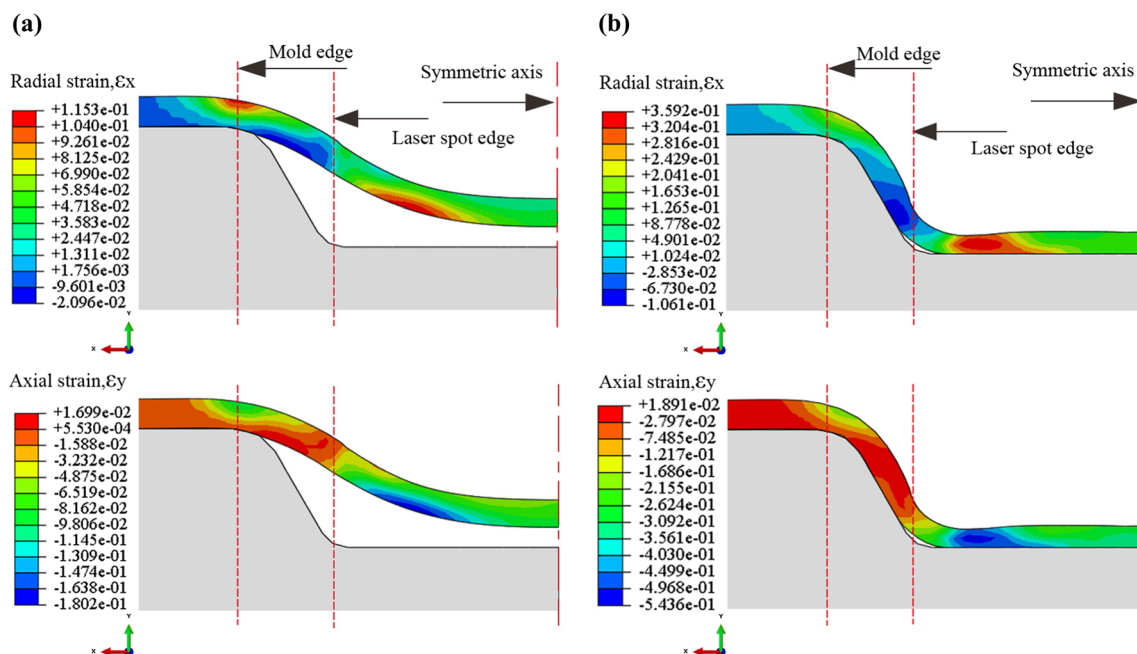
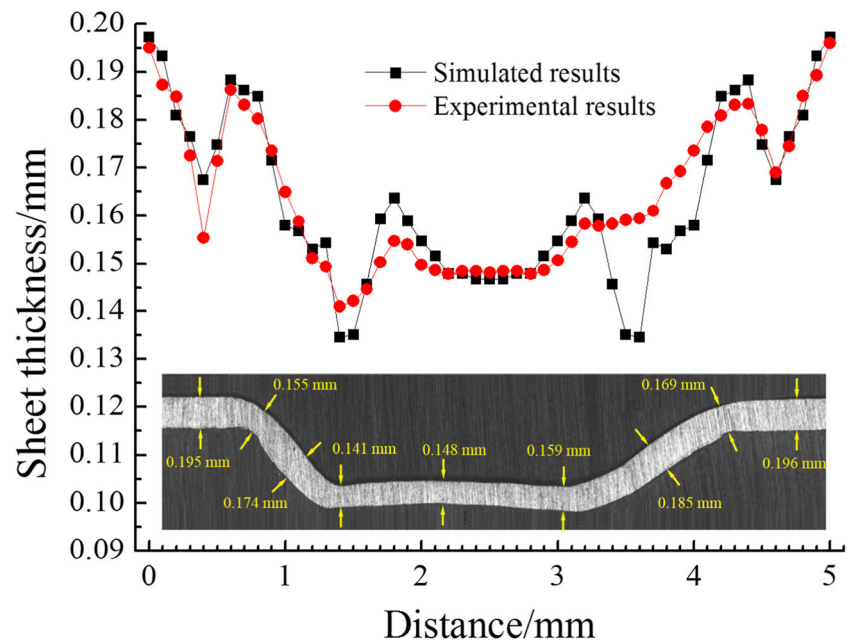


Fig. 7 Plastic strains of sheet impacted by laser with power density 2.34 GW/cm^2 . **a** at the end of solution time 1860 ns; **b** at the end of solution time 10,000 ns

Fig. 8 The thickness distribution of central cross section



thickness is reduced at this region. Once the sheet fits the mold cavity, the material of sheet at most places stops moving, but the material near the bottom corner of mold cavity does not stop moving immediately owing to inertia effect, which continues to be stretched for a while and fills the corner. The material at other regions in sheet does not flow easily into the corner because of the contact friction between metal sheet and the mold. Hence, the thickness of the sheet near the bottom corner of mold is greatly reduced. The location of maximum thickness thinning in current case seems different from that in μ LDF illustrated by Gao et al. [11]. During μ LDF, the metal sheet within blank holder is constrained, and the material at the entrance of mold cavity is subjected to stronger stress due to severe bending and stretching, so the thickness of metal sheet at this region is reduced more easily in comparison with its neighboring regions, and the localized necking is often found at the entrance of mold, which has been validated by references [11, 24]. Due to the complicated interaction among shock waves, metal sheet and mold, the mechanism of thickness reduction still needs further investigations in the future.

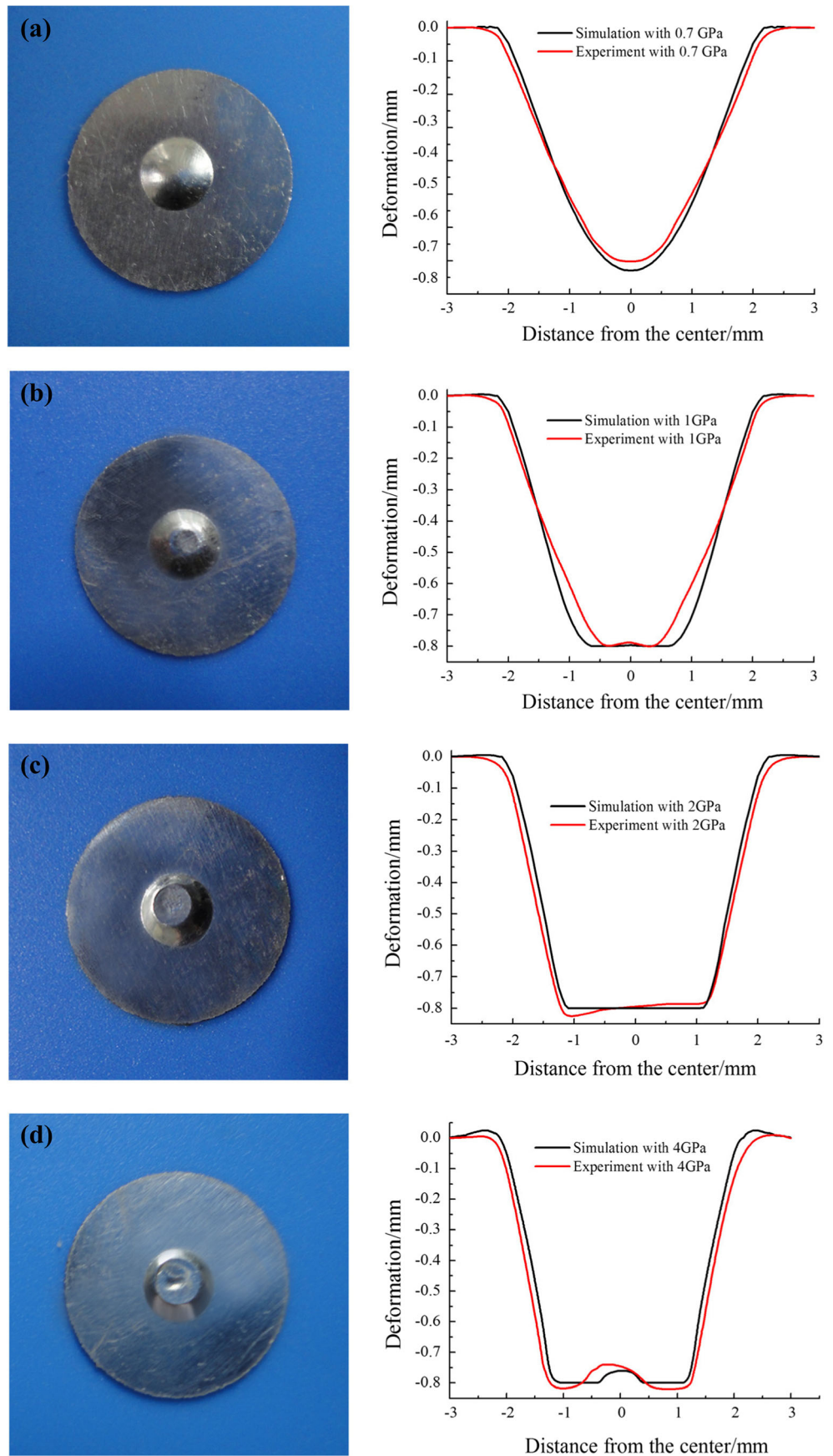
Effect of shock wave pressure

In order to verify the effect of shock wave pressure on sheet plastic deformation, we take into consideration pressures, 0.7, 1, 2 and 4 GPa, which are corresponding to laser densities, 0.29, 0.59, 2.34 and 9.36 GW/cm² respectively. Figure 9 shows a series of shaped conical cups, and also displays their cross-sectional profiles. From Fig. 9, it can be seen that the profiles of formed cups are somewhat different and their

shapes change with increase in pressure of applied shock wave.

When metal sheet is loaded by shock wave with pressure 0.7 GPa, it is deformed into the cup with a hemispherical bottom, because the loaded pressure is too low to push the sheet to impact upon the mold bottom cavity. Under this circumstance, the mold mainly plays a role in supporting and controlling the 2D the shape of deformed part, which is the same as that obtained from 2D LSF [8–10]. When the sheets are imposed by pressure 1, 2 and 4 GPa respectively, they turn into the conical cups with flat bottom resulted from the collision with cavity bottom. Moreover, with the applied pressure increasing from 1 to 2 GPa, the area of flat bottom enlarges accordingly. As mentioned above in “Velocity and momentum” section, a higher pressure can transfer more momentum to the sheet and to raise its initial velocity. The raised velocity leads to severe collision and further results in squeezing more material flowing transversely toward the outskirts of the cavity bottom to fill the corner of mold cavity bottom. As a consequence, the higher pressure leads to enlarging contact area between the deformed sheet and the mold, which reflects the sheet forming precision. Therefore, the properly increased pressure of applied shock wave is beneficial to improve the forming precision. Nevertheless, too high pressure exerts an unfavorable effect on the forming precision, since there is reverse plastic deformation other than failure in 2D LSF [25], which results from the violent collision produced by too high pressure, for example the sheet loaded by 4 GPa pressure. The phenomenon of rebound at the central part formed by micro-LSF was also reported by Li and Cheng

Fig. 9 Geometric shape of the part shocked by pressure **a** 0.7GPa; **b** 1GPa; **c** 2GPa; **d** 4GPa



[12], and they thought that it was attributed to a large resistance force of the compressed air applied on the bottom of the sample as the metal sheet deformed into the mold at a high velocity. The conclusion may be right when the cone-shaped mold is used, since the air can be compressed gradually into the tip of the cone and gathered there. But the conclusion can not be applied to the flat bottom of mold cavity in current case, so the central region of metal sheet moves with the fastest speed and first collides with mold cavity, and the compressed air is discharged from the vent at the bottom of the mold. The resident reverse deformation increases the flatness error of the bottom and reduces the forming precision. Therefore, in order to obtain higher forming precision, a suitable pressure of shock wave is required.

Conclusions

Laser shock forming Al alloy 2024-T351 sheet with mold was investigated with both numerical and experimental methods. A finite element model had been established, and some deforming behaviors were predicted. The effect of shock wave pressure on sheet forming precision was also investigated. The simulated results were verified with a series of experiments. Some important findings could be obtained as follows:

- (1) When the 0.2 mm thick sheet is subjected to laser shock wave with pressure 2 GPa, the maximum downward velocity of metal sheet is up to 614 m/s. After collision with the mold cavity, the rebound velocity runs up to 319 m/s.
- (2) The flat metal sheet can be formed by shock wave into a conical cup with a flat bottom. The wall thickness of the formed cup is non-uniform, and the greatest amount of localized thinning occurs at the corner region of mold cavity bottom.
- (3) During LSF, too high pressure cannot shape the sheet well owing to the resident reverse deformation at the central region of bottom, and too low pressure cannot form sheet well either. In order to obtain the formed parts with high precision, an appropriate pressure is required.

Compliance with ethical standards

Funding This study was founded by the National Natural Science Foundation of China (grant number: 51175002, 51675002) and State Key Laboratory of Materials Processing and Die & Mould Technology, Huazhong University of Science and Technology (grant number: P2017-007).

Conflict of interest All authors declare that we have no conflict of interest.

References

1. Mamutov AV, Golovashchenko SF, Mamutov VS (2015) Modeling of electrohydraulic forming of sheet metal parts. *J Mater Process Technol* 219:84–100
2. Mousavi SAAA, Riahi M, Parast AH (2007) Experimental and numerical analyses of explosive free forming. *J Mater Process Technol* 187–188:512–516
3. Zhang X, Wang ZR, Song FM, Yu LZ, Lu X (2004) Finite element simulation of the electromagnetic piercing of sheet metal. *J Mater Process Technol* 151:350–354
4. Karimi A, Niayesh K, Bahmani MA (2010) Magnetic filed enhancement in electromagnetic forming systems using anisotropic materials. *Int J Mater Form* 3(3):205–208
5. Zhou M, Zhang YK, Cai L (2002) Laser shock forming on coated metal sheets characterized by ultrahigh-strain-rate plastic deformation. *J Appl Phys* 91(8):5501–5503
6. Carr AR, Walker A, Combaz E (2015) Derivation of a forming limit stress diagram from an experimental FLC, and comparison of the two criteria when applied to FE simulation of a pressing using different yield functions. *Int J Mater Form* 8(1):45–57
7. Sigvant M, Mattiasson K, Vegter H, Thilderkvist P (2009) A viscous pressure bulge test for the determination of a plastic hardening curve and equibiaxial material data. *Int J Mater Form* 2(4):235–242
8. Niehoff HS, Vollertsen F (2005) Non-thermal laser stretch-forming. *Adv Mater Res* 6–8:433–440
9. Cheng GJ, Pirzada D, Ming Z (2007) Microstructure and mechanical property characterizations of metal foil after microscale laser dynamic forming. *J Appl Phys* 101(6):063108
10. Zhang XQ, She JP, Li SZ, Duan SW, Zhou Y, Yu XL, Zheng R, Zhang B (2015) Simulation on deforming progress and stress evolution during laser shock forming with finite element method. *J Mater Process Technol* 220:27–35
11. Gao H, Ye C, Cheng GJ (2009) Deformation behaviors and critical parameters in microscale laser dynamic forming. *J Manuf Sci Eng* 131(5):051011
12. Li J, Cheng GJ (2010) Multiple-pulse laser dynamic forming of metallic thin films for microscale three dimensional shapes. *J Appl Phys* 108(1):013107
13. Jiang YF, Huang Y, Jin H, Gu YY, Ren AG, Huang LW, Qian XM (2013) Research on precision control of sheet metal forming by laser shock waves with semi-die. *Opt Laser Technol* 45(1):598–604
14. Shen ZB, Liu HX, Wang X, Wang CT (2016) Improving the forming capability of laser dynamic forming by using rubber as a forming medium. *Appl Surf Sci* 369:288–298
15. Fabbro R, Fournier J, Ballard P, Devaux D, Virmont J (1990) Physical study of laser-produced plasma in confined geometry. *J Appl Phys* 68(2):775–784
16. Zhang WW, Yao YL (2002) Micro scale laser shock processing of metallic components. *J Manuf Sci Eng* 124(2):369–378
17. Johnson GR, Cook WH (1983) A constitutive model and data for metals subjected to large strains, high strain rates and high temperatures. *Proceedings of the 7th ISB*: pp. 541–547
18. Ocaña JL, Correa C, García-Beltrán A, Porro JA, Díaz M, Ruiz-de-Lara L, Peral D (2015) Laser shock processing of thin Al2024-T351 plates for induction of through-thickness compressive residual stresses fields. *J Mater Process Technol* 223:8–15
19. Gill AS, Telang A, Vasudevan VK (2015) Characteristics of surface layers formed on inconel 718 by laser shock peening with and without a protective coating. *J Mater Process Technol* 225:463–472
20. Jorgensen DJ, Pollock TM, Begley MR (2015) Dynamic response of thin films on substrates subjected to femtosecond laser pulses. *Acta Mater* 84:136–144

21. Guglielmotti A, Quadrini F, Squeo EA, Tagliaferri V (2009) Diode laser bending of tongues from slotted steel tubes. *Int J Mater Form* 2(2):107–111
22. Mohammadi A, Vanhove H, Bael AV, Duflou JR (2016) Towards accuracy improvement in single point incremental forming of shallow parts formed under laser assisted conditions. *Int J Mater Form* 9(3):339–351
23. Peyre P, Berthe L, Scherpereel X, Fabbro R (1998) Laser-shock processing of aluminium-coated 55C1 steel in water-confinement regime, characterization and application to high-cycle fatigue behaviour. *J Mater Sci* 33(6):1421–1429
24. Zheng C, Sun S, Ji Z, Wang W, Liu J (2010) Numerical simulation and experimentation of micro scale laser bulge forming. *Int J Mach Tools Manuf* 50(12):1048–1056
25. Wang X, Ma YJ, Shen ZB, Gu YX, Zhang D, Qiu TB, Liu HX (2015) Size effects on formability in microscale laser dynamic forming of copper foil. *J Mater Process Technol* 220:173–183